# A Non-Stationary Errors-in-Variables Method with Application to Mineral Exploration

K. Lau [1] J. H. Braslavsky J. C. Agüero G. C. Goodwin

*ARC Centre for Complex Dynamic Systems and Control, The University of Newcastle, Callaghan, NSW, 2308, AUSTRALIA.*

**Abstract**

In this paper, a non-stationary errors-in-variables (EIV) model estimation method is proposed and applied to the problem of model estimation for noise-cancellation in transient electromagnetic mineral exploration. Alternative methods for noise cancellation in these systems rely on specific signal characteristics, and are thus less readily transferable to other applications. The proposed method produces a model that agrees well with those obtained by alternative methods and has similar noise cancellation performance. This is shown by performance comparisons on experimental data.

*Key words:* Errors-in-variables identification

## 1 Introduction

This paper is concerned with identifiability and model estimation for a class of non-stationary errors-in-variables systems. An estimation method for this class of systems is proposed and applied to a problem arising in mineral exploration.

An errors-in-variables (EIV) system is one in which both the input and output are subject to measurement noise. A typical EIV system is shown in Fig. 1. From the figure, we have

$$u(k) = u_0(k) + n_1(k), \quad (1)$$
$$y(k) = y_0(k) + n_2(k), \quad (2)$$

where $u(k)$ and $y(k)$ are the measured input and output, $u_0(k)$ and $y_0(k)$ are the true input and output, and $n_1(k)$ and $n_2(k)$ are the measurement noise sequences. The transfer function from $u_0(k)$ to $y_0(k)$ is denoted by $G_o(z)$.

We introduce the following notation. Let $x$ and $z$ be two signals. Then $\Phi_{xx}(\omega)$ denotes the (auto) power spectral density (PSD) of $x$ and $\Phi_{xz}(\omega)$ denotes the cross power spectral density (CPSD) $x$ and $z$. We refer to PSDs and CPSDs, collectively, as spectra. A 'hat' $\hat{}$ is use to denote an estimated quantity (e.g., $\hat{G}(e^{j\omega})$, $\hat{\Phi}_{uy}(\omega)$).

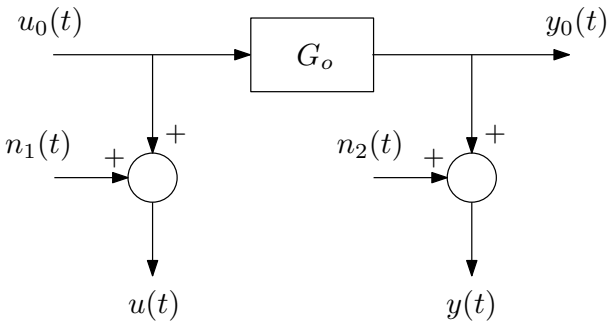


Fig. 1. An errors-in-variables system.

The presence of errors-in-variables has implications for model estimation. For example, it is known that ignoring the noise on the input may lead to biased estimates of the model. It is also known that EIV systems are in general not uniquely identifiable from second order properties. These two topics are discussed in more detail below.

We first discuss estimation bias. Consider the estimate

*Email addresses:* K.Lau@newcastle.edu.au (K. Lau), Julio.Braslavsky@newcastle.edu.au (J. H. Braslavsky), Juan.Aguero@newcastle.edu.au (J. C. Agüero), Graham.Goodwin@newcastle.edu.au (G. C. Goodwin).

[1] Corresponding author.

of the frequency response given by

$$\hat{G}_{\text{naive}}(e^{j\omega}) = \frac{\hat{\Phi}_{yu}(\omega)}{\hat{\Phi}_{uu}(\omega)}. \quad (3)$$

We assume that $\hat{\Phi}_{yu}(\omega)$ and $\hat{\Phi}_{uu}(\omega)$ are consistent estimates of $\Phi_{yu}(\omega)$ and $\Phi_{uu}(\omega)$. The estimate given by (3) is known as the unrealisable Wiener filter (Söderström, 2002). Here, we refer to this method of estimating the frequency response as the 'naive method' (as it implicitly ignores the noise on the input). We observe that

$$\frac{\Phi_{yu}(\omega)}{\Phi_{uu}(\omega)} = \frac{G_o(e^{j\omega})\Phi_{u_0u_0}(\omega)}{\Phi_{u_0u_0}(\omega) + \Phi_{n_1n_1}(\omega)}. \quad (4)$$

Equation (4) (together with the assumption of consistent spectral estimates) implies that the estimate $\hat{G}_{\text{naive}}(e^{j\omega})$ is asymptotically unbiased if and only if $\Phi_{n_1n_1}(\omega) = 0$ i.e., there is no measurement noise on the input. When this is not the case, the method yields a biased estimate. Furthermore, since $\Phi_{u_0u_0}(\omega) > 0$ and $\Phi_{n_1n_1}(\omega) > 0$, then we see from the above equation that the naive method under-estimates the gain.

We now discuss the problem of identifiability. It is well known that EIV models are not generally identifiable from second order properties (Agüero and Goodwin, 2008b) when the noise parameters are unknown. By this we mean that EIV systems cannot be uniquely determined using only knowledge of the input and output spectra. The identifiability problem can be resolved by imposing additional assumptions (e.g., knowledge of the ratio of the noise variances). A recent review of EIV identification techniques, and the assumptions required in each case is given in Söderström (2007).

The analysis of identifiability is closely related to model estimation because identifiability is often established by constructing an algorithm for inferring the model from the (true) input and output spectra. An estimation method (algorithm) can then be obtained by substituting estimates of the spectra for the true spectra.

The identifiability of stationary EIV dynamic systems has been studied in Anderson and Deistler (1984); Anderson (1985); Deistler (1986) under very general conditions. Related results are also given in Agüero and Goodwin (2008b). The use of non-stationary data to resolve identifiability has a long history for the static case (Wald, 1940). More recently, Markovsky et al. (2006) have extended the idea to special cases of the dynamic problem. These results are also discussed in Söderström (2007).

In this paper, we consider a class of (non-stationary) errors-in-variables system in which the spectra of the input and output changes with time. We first establish conditions for identifiability and then propose a model estimation method.

The motivation for the work presented here is a problem encountered in transient electromagnetic (TEM) mineral exploration. The problem is to estimate a model for use in noise cancellation. In this application, errors-in-variables arise because the input is measured in the presence of noise. The current authors in a recent paper (Lau et al., 2007) proposed a method for mitigating the effect of EIV by utilising specific knowledge of the input signal characteristics. However, these characteristics are problem specific and thus the associated approach is not readily transferable to other applications.

In this paper, we apply the proposed method to the problem of estimating a model for the application described above. The results are validated against models found using two independent methods (including the one proposed in Lau et al. (2007)). It is shown that the estimated response found by the method proposed here agrees well with those found using the alternative methods. In addition, the fitted model performs equally well when used for noise cancellation. This indicates that the method can be successfully applied in this case, and suggests that the approach could be useful in other EIV applications.

The layout of the remainder of the paper is as follows: In Sect. 2, we provide background information on TEM surveying and sferics noise. Then, in Sects. 3 and 4, we introduce the EIV problem and present the non-stationary EIV method that we will subsequently deploy. We also provide the identifiability result on which the proposed method is based. We apply the EIV method and validate the estimated models in Sect. 5. Conclusions are drawn in Sect. 6. A preliminary version of these results was presented in Lau et al. (2008).

## 2 Background to TEM Surveying and Sferics

### *2.1 TEM surveying*

Transient electromagnetic surveying (also known as time-domain electromagnetic surveying) is a technique used in mineral exploration to detect underground conductive ore bodies by the induction and detection of electromagnetic (EM) fields (Kearney et al., 2002). Here, we will be concerned with ground-based transient electromagnetic (TEM) surveying using a system known as Geoferret$^{\text{TM}}$(Carter, 2005). Fig. 2 shows a typical system configuration for TEM surveying using this system.

The typical operation of a TEM surveying system consists of two phases: firstly, the transmission of a *primary field*, during which no measurements are made, and secondly, after the transmitter is switched off, the detection of the *secondary field* response (i.e., the transient response) of the earth. To generate the primary field, a pulsed current waveform is passed through a loop or coil of wire (the transmitter), which is laid on the surface of

the area to be surveyed. The time-varying primary field induces (eddy) currents in the ground beneath the transmitter, which in turn induce currents at greater depths in conductive ore bodies, if present. The induced currents produce a secondary magnetic field which decays when the transmitter is switched off (in between the current pulses). The vertical component of the decaying field is measured by an array of receiving antennae (sensors) on the surface of the earth. The magnitude and rate of decay of the field depends on the electrical conductivity of the ground, and, through posterior signal processing, allows the identification and location of target ore bodies at depths of up to 500 m.

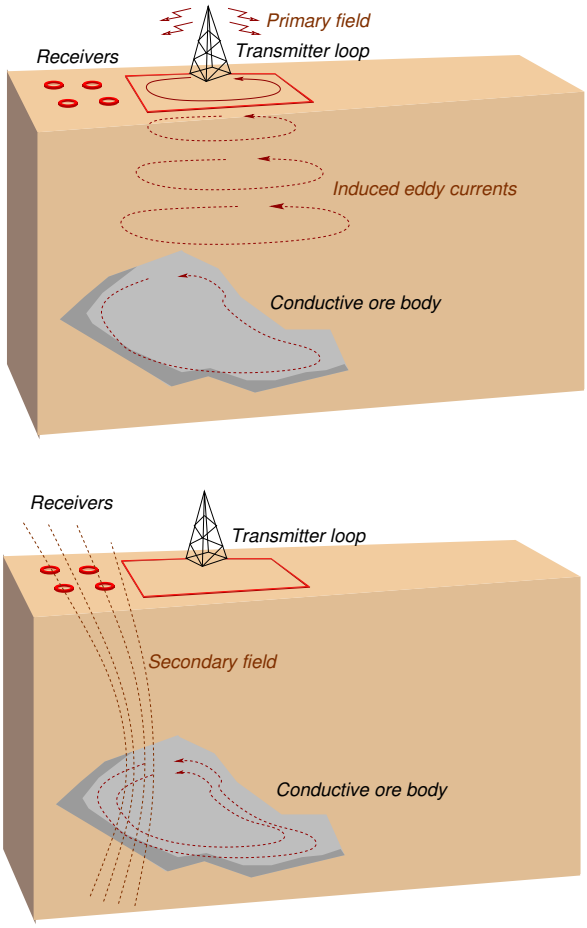


Fig. 2. Typical ground-based TEM surveying system configuration. (Top) A primary field is first generated by passing a pulsed current waveform through a loop of wire. (Bottom) The primary field induces currents in the earth which, in turn, produce a secondary magnetic field. An array of sensors is used to measure the transient response of the (decaying) secondary field in between the current pulses.

We consider a system in which the transmitter loop is of the order of 1 km$^2$ in area, and the receiving antennae have a diameter of approximately 1 m. The antennae spacing is typically 50–100 m. The periodic current waveform which is injected into the transmitter consists of a series of square pulses of alternating sign. The amplitude of the current pulses is approximately 20 A, and the magnitude of the primary field at the centre of the transmitter loop is approximately 7 nT. The secondary field at different locations is measured using a number of receiving antennae. The measured data is then interpreted to obtain a geological model which is consistent with the data.

A more detailed description of TEM surveying can be found in Nabighian and Macnae (1991) and *Geophysical Exploration for Engineers* (U.S. Army (1998)).

### *2.2 Sources of noise*

In TEM surveying, the useable detection depth and the types of minerals which can be detected are dependent on the signal-to-noise ratio. Hence, it is of interest to reduce the amount of noise. Sources of noise include instrument noise, environmental noise and harmonic disturbances (including 50 Hz power line interference). Another source of noise is 'wind noise', i.e., low frequency ($< 10$ Hz) noise due to small movements of the antenna relative to the (static) magnetic field of the earth. In the next section, we describe an important source of environmental noise referred to as 'sferics'.

### *2.3 Sferics noise*

One of the major sources of noise in the detection of deep underground ore bodies is sferics: environmental EM radiation that dominates receiver instrument noise in some environments (such as close to the equator, where thunderstorms frequently occur). Sferics (short for 'atmospherics') originate from the EM radiation produced by lightning strikes. These EM signals can travel thousands of kilometres through the space between the earth and the ionosphere, which acts as a waveguide. Hence, local and distant lightning storms contribute to the sferics noise measured at any single point.

Sferics noise can be divided into two groups; local (near-field) and distant (far-field). Local sferics noise consists of large, infrequent, bursts of short pulses. (It is impulsive and is non-stationary in nature.) Fig. 3 shows a large measured sferic occurring at approximately 0.002 s. Distant sferics noise may be characterised as coloured noise. It has been estimated that there are approximately $44 \pm 5$ lightning strikes per second worldwide (Christian et al., 2003). Thus, distant sferics noise consists of many small pulses and can be considered to be quasi-stationary. The spectrum of sferics noise is concentrated in the 1–500 Hz and 2.5–10 kHz frequency bands. The dip in the spectrum between 500 Hz and 2.5 kHz is due to the attenuation of the earth-ionosphere waveguide at these frequencies.

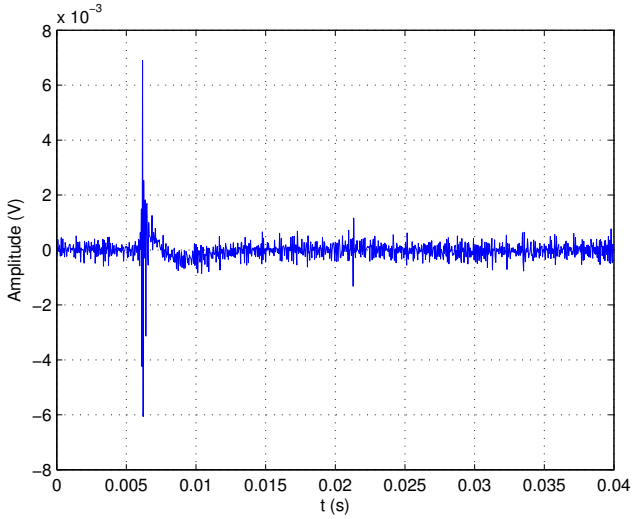


Fig. 3. A measured large sferic.

## 3 Sferics Noise Cancellation and EIV

One way of reducing the effect of sferics is to perform noise cancellation from one receiving antenna to another. We refer to these antennae, respectively, as the reference antenna and the output antenna. The reference antenna is placed at a remote location, so that the effect of the transmitted signal is negligible. The technique utilises the fact that the sferics measured at different locations are affected by local geological conditions but are correlated.

In order to perform noise cancellation one needs to find a model relating the sferics measured at the reference and output antennae. We do this by estimating a model from 'noise-only' measurements taken at the two antennae with the transmitter turned off. In this context, the components of the measurements due to sferics noise are considered to be the true *signals*, and the rest of the components are considered to be measurement noise. The system can be formulated as an EIV system of the form shown in Fig. 1 with the following signal definitions:

| | |
|---|---|
| $u$ | measured signal at the reference antenna |
| $u_0$ | the sferics component of $u$ |
| $n_1$ | the non-sferics components of $u$ |
| $y$ | measured signal at the output antenna |
| $y_0$ | the sferics component of $y$ |
| $n_2$ | the non-sferics components of $y$ |

Fig. 5 in Sect. 5 shows some typical power spectral densities (PSDs) for noise-only measurements collected using the Geoferret system. We observe that there is a large noise mound between approximately 10 and 600 Hz. This part of the spectrum can be attributed to sferics noise. The size of the mound varies with time due to the non-stationarity of local sferics.

Here, we focus on reducing the noise spectrum between 10 and 600 Hz for the following reasons:

- It is known from the literature (see Sect. 2.3) that sferics have significant power in this frequency band.
- We are particularly interested in the cancellation of noise at low frequencies, which are the most relevant to the detection of the response from target ore bodies.

We concentrate on the reduction of the 'baseline' noise spectrum, not the harmonic components. The latter components can be removed separately.

We can verify that medium- to near-field sferics make a significant contribution to the baseline noise between 10 and 600 Hz by filtering the signal to remove the harmonic disturbances (Sect. 2.3) and the components outside this frequency range. The resultant signal corresponds to the baseline component of the noise in the 10 to 600 Hz frequency band. Fig. 4 shows the filtered version of the sferic from Fig. 3. It can be seen that, in the above frequency band, the sferics pulse is large relative to the measurement noise.

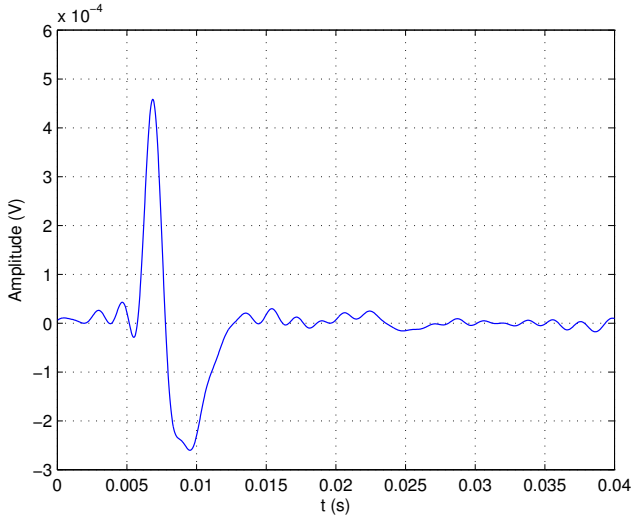


Fig. 4. Filtered version of the sferic in Fig. 3.

## 4 The Non-Stationary EIV Method

In this section, we consider a class of EIV systems in which the data exhibit two different behaviors on two non-overlapping time intervals. The EIV system associated with the sferics noise cancellation problem belongs to this class of systems because the sferics signal is non-stationary. We first analyze identifiability and then propose an estimate obtained from this analysis. A preliminary version of these results was presented in the conference paper Agüero and Goodwin (2008a).

In the discussion that follows, we refer to the two behaviors (time intervals) as scenario A and scenario B. We also use the subscripts 'A' and 'B' to denote signals corresponding to scenarios A and B, respectively.

We assume that each scenario can be modelled as follows:

$$\begin{aligned} y_i(t) &= G_{oi}u_{oi}(t) + n_{2i}(t) \\ u_i(t) &= u_{oi}(t) + n_{1i}(t) \end{aligned} \tag{5}$$

where the index $i \in \{A, B\}$ represents the corresponding scenario.

We also assume the following:

**Assumption 1** *The input-output spectra for both scenarios, A and B, are available.*

We now present a theorem which analyzes the identifiability of an EIV system, of the type given in (5), from data obtained from two scenarios. The theorem uses subsets of the following additional assumptions:

**Assumption 2** *The process is the same for both scenarios:* $G_{o\,A} = G_{o\,B} = G_o$.

**Assumption 3** *The input noise spectrum is the same for both scenarios:* $\Phi_{n_{1A}n_{1A}}(\omega) = \Phi_{n_{1B}n_{1B}}(\omega) = \Phi_1$.

**Assumption 4** *The output noise spectrum is the same for both scenarios:* $\Phi_{n_{2A}n_{2A}}(\omega) = \Phi_{n_{2B}n_{2B}}(\omega) = \Phi_2$.

**Assumption 5** *The input* $u_o$ *has the same second order properties for every experiment:* $\Phi_{u_{0A}u_{0A}}(\omega) = \Phi_{u_{0B}u_{0B}}(\omega) = \Phi_0$.

**Theorem 6** *The EIV system given in* (5) *is identifiable from data coming from two different scenarios, A, and B, if any of the following conditions hold:*

- *(i) Assumptions 1, 2 and 3 hold, and* $\Phi_{u_{0A}u_{0A}}(\omega) \neq \Phi_{u_{0B}u_{0B}}(\omega)$ *(a.e.),*
- *(ii) Assumptions 1, 2 and 4 hold, and* $\Phi_{u_{0A}u_{0A}}(\omega) \neq \Phi_{u_{0B}u_{0B}}(\omega)$ *(a.e.),*
- *(iii) Assumptions 1, 4 and 5 hold, and* $G_{o\,A} \neq G_{o\,B}$ *(a.e.),*
- *(iv) Assumptions 1, 3, 4 hold, and* $\tilde{\Phi}_u\tilde{\Phi}_y < 0$, $\forall\omega$, *where* $\tilde{\Phi}_u = \Phi_{u_Au_A}(\omega) - \Phi_{u_Bu_B}(\omega)$ *and* $\tilde{\Phi}_y = \Phi_{y_Ay_A}(\omega) - \Phi_{y_By_B}(\omega)$,

*where a.e. stands for almost everywhere.*

***PROOF.*** *Our strategy will be to retrieve* $G_{o\,i}$ *from the input and output PSDs and CPSD from both scenarios A and B. Once* $G_{o\,i}$ *has been obtained* $\Phi_{u_{0\,i}u_{0\,i}}(\omega)$, $\Phi_{n_{1\,i}n_{1\,i}}(\omega)$, $\Phi_{n_{2\,i}n_{2\,i}}(\omega)$, $i = A, B$ *can be retrieved as follows:*

$$\hat{\Phi}_{u_{0\,i}u_{0\,i}}(\omega) = \frac{\Phi_{y_iu_i}(\omega)}{G_{o\,i}} \tag{6}$$

$$\hat{\Phi}_{n_{1\,i}n_{1\,i}}(\omega) = \Phi_{u_iu_i}(\omega) - \hat{\Phi}_{u_{0\,i}u_{0\,i}}(\omega) \tag{7}$$

$$\hat{\Phi}_{n_{2\,i}n_{2\,i}}(\omega) = \Phi_{y_iy_i}(\omega) - |\hat{G}_{o\,i}|^2\hat{\Phi}_{u_{0\,i}u_{0\,i}}(\omega) \tag{8}$$

**(i)** *In this case we have that* $G_o$ *and* $\Phi_{n_1n_1}(\omega)$ *are the same for both scenarios. Then, the input-output and input spectrum for the two scenarios are given by:*

$$\Phi_{y_iu_i}(\omega) = G_o\Phi_{u_{0\,i}u_{0\,i}}(\omega), \quad \Phi_{u_iu_i}(\omega) = \Phi_{u_{0\,i}u_{0\,i}}(\omega) + \Phi_1$$

*Thus, we have that* $G_o$ *can be retrieved as follows*

$$G_o = \frac{\Phi_{y_Au_A}(\omega) - \Phi_{y_Bu_B}(\omega)}{\Phi_{u_Au_A}(\omega) - \Phi_{u_Bu_B}(\omega)} \tag{9}$$

*Notice that we need* $\Phi_{u_Au_A}(\omega) \neq \Phi_{u_Bu_B}(\omega)$ *(or equivalently* $\Phi_{u_{0A}u_{0A}}(\omega) \neq \Phi_{u_{0B}u_{0B}}(\omega)$*) almost everywhere (a.e.). The proofs of (ii), (iii) and (iv) are given in Agüero and Goodwin (2008a).* □

In the case of the sferics model estimation problem, the sferics signal ($u_0$) is non-stationary, but the process and the noise spectra do not change with time. Thus from condition (i) of the above Theorem, the system is identifiable provided that $\Phi_{u_{0A}u_{0A}}(\omega) \neq \Phi_{u_{0B}u_{0B}}(\omega)$ (a.e.). It then follows from Equation (9) that an estimate of $G_o$ is given by

$$\hat{G}_{\mathrm{EIV}}(e^{j\omega}) = \frac{\hat{\Phi}_{y_Au_A}(\omega) - \hat{\Phi}_{y_Bu_B}(\omega)}{\hat{\Phi}_{u_Au_A}(\omega) - \hat{\Phi}_{u_Bu_B}(\omega)}. \tag{10}$$

In the following sections, we explore the use of estimate (10) as a model for sferics noise cancellation.

## 5 Application of the Non-stationary EIV Method to Model Estimation for Sferics Noise Cancellation

In this section, we use the non-stationary EIV method described above to estimate the model from a reference antenna to an output antenna.

The method is tested using two 60 s intervals of (experimental) data that have noticeable differences in spectra. For this experiment, the distance between the reference and output antennae was approximately 4 km. The data

was sampled at a rate of 25 kHz. We let $u_A$ and $y_A$ correspond to the first interval of the data and let $u_B$ and $y_B$ correspond to the second interval.

Fig. 5 shows the PSDs of $u_A$, $u_B$, $y_A$ and $y_B$. It can be seen that there is a difference in the PSDs for sections A and B of the data in the region of interest (i.e., the mound between 10 and 600 Hz). As mentioned in Sect. 3, this is due to the non-stationary nature of local sferics.

Fig. 6 shows the magnitude of the estimated frequency response when the non-stationary EIV method (Equation (10)) is used to calculate the response. The response is shown between 10 and 600 Hz. The figure also shows the biased estimate $\hat{G}_{\text{naive}}(e^{j\omega})$ obtained by ignoring the measurement noise on the input and using (3) to estimate the response. From the figure, it can be seen that the EIV and naive methods yield very different frequency responses. In particular, the magnitude of the naive estimate is less than the magnitude of the EIV estimate (at most frequencies). This is consistent with the observation, made in the introduction, that the naive method under-estimates the gain. In the sections that follow, we confirm that the EIV method results in a better model of the system.

We notice that, in Fig. 6, the estimate using the non-stationary EIV method has a much larger variance than the biased (naive) estimate. This is due to the ratio calculated in (10) and due to harmonic components. The EIV method assumes that the CPSDs and PSDs of the harmonic components in sections A and B of the data cancel exactly. If the harmonics are large, then small errors in the cancellation can result in large errors in the estimated gain. Since the harmonic disturbances appear as outliers in the (C)PSDs, we remove them by applying a median filter (a form of outlier rejection) to the (C)PSDs. We then fit a first order biproper model (relative degree 0) to the resulting frequency response.

### *5.1 Comparison to a model found using time and frequency selectivity*

Fig. 7 shows the estimated frequency responses (with the outliers removed) for the EIV and naive methods. The responses of the fitted first order models are also plotted. We validate these responses against a model found using the approach described in Lau et al. (2007) and summarised below. It is clear that the non-stationary EIV method provides a model which is closer to the validation model than the model obtained using the naive method.

The validation model is found by exploiting time and frequency selectivity to isolate a part of the input with a high signal to noise ratio. The procedure can be summarised as follows: A filter with a passband between 10 and 600 Hz and notches at the harmonic frequencies is

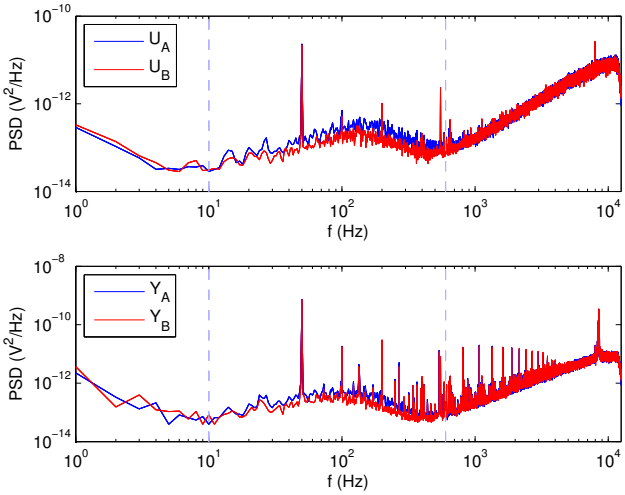


Fig. 5. PSDs of the signals used to estimate the frequency response using the non-stationary EIV method. (Top) PSDs of $u_A$ and $u_B$. (Bottom) PSDs of $y_A$ and $y_B$.

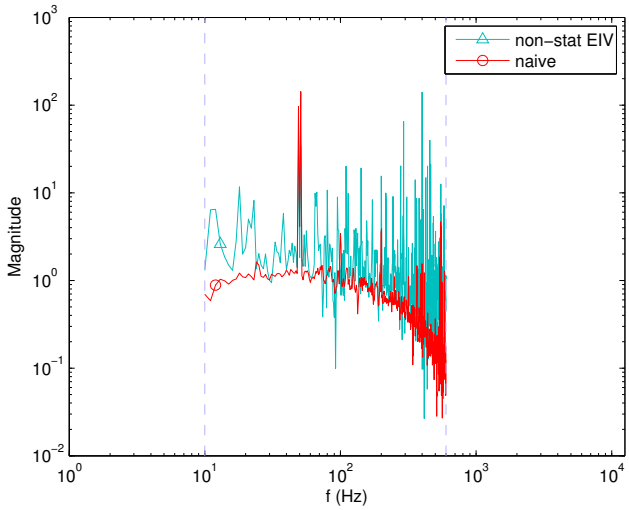


Fig. 6. Estimated frequency responses (magnitude only) using the non-stationary EIV and naive methods.

applied to the input and output data. In the filtered signals, the sferics appear as large pulses which stand out from the filtered noise. We fit a model to a 'marked sferic', a short section of the filtered data containing a large sferic (and hence, a high signal to noise ratio). An example of a marked sferic is given in Fig. 4. We refer to this method of finding a model as the 'marked data' method. More details can be found in Lau et al. (2007). As noted in the Introduction, this validation method uses specific knowledge regarding this particular application.

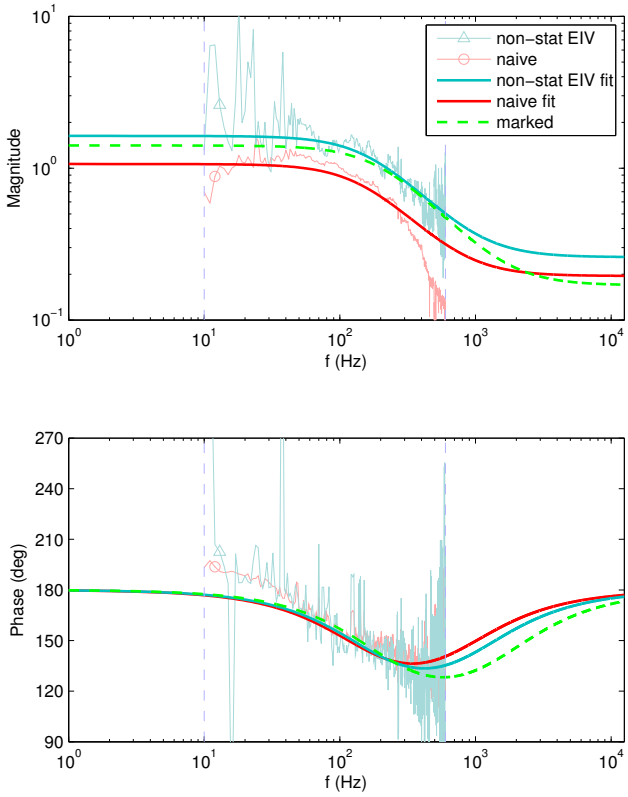


Fig. 7. Comparison of the frequency responses (magnitude and phase) found using the non-stationary EIV and naive methods to the model found using marked data. The estimated responses with outlier rejection and the responses of the fitted models for the non-stationary EIV and naive methods are shown.

### 5.2 *Comparison to a model found using an independent output measurement*

For a second validation test we utilise measurements from an independent output antenna. Let $v(k)$ be the measured output, $v_0(k)$ be the true output, $n_3(k)$ be the measurement noise, and $G_v(z)$ be the transfer function from $u_0(k)$ to $v_0(k)$. We have

$$v(k) = v_0(k) + n_3(k).$$

It can be easily shown that, if $\hat{\Phi}_{yv}(\omega)$ and $\hat{\Phi}_{uv}(\omega)$ are consistent estimates of the corresponding CPSDs, then an unbiased estimate of $G_o(e^{j\omega})$ is given by

$$\hat{G}_{\text{indep}}(e^{j\omega}) = \frac{\hat{\Phi}_{yv}(\omega)}{\hat{\Phi}_{uv}(\omega)}. \tag{11}$$

We refer to this method as the independent output method.

The frequency responses obtained using the non-stationary EIV method and independent output method are compared in Fig. 8. We again see that responses found using the EIV method agree well with the validation method.

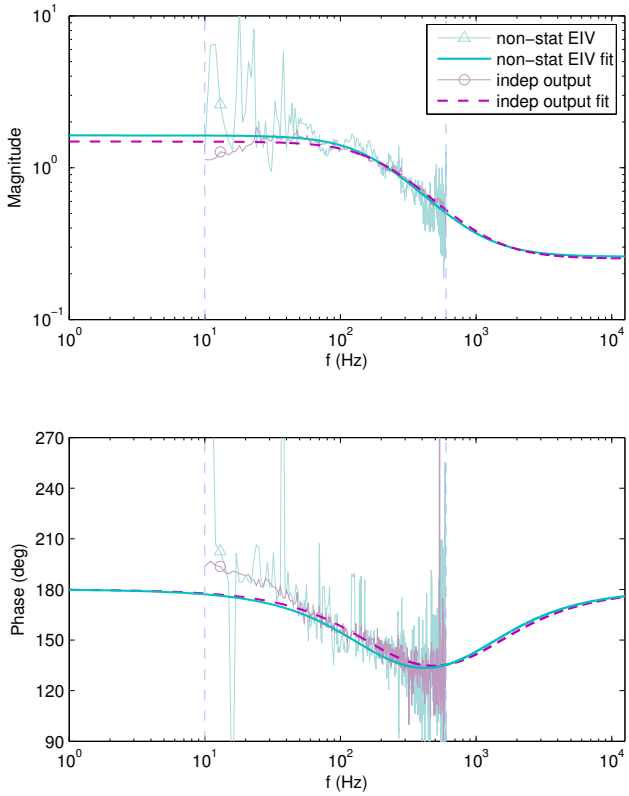


Fig. 8. Comparison of the frequency responses (magnitude and phase) found using the non-stationary EIV method and the independent output method. The estimated frequency responses with outlier rejection and the responses of the fitted models for the two methods are shown.

### 5.3 *Comparison of noise cancellation performance*

For a final validation test, we compare the noise cancellation performance of the models found using all four methods described above (non-stationary EIV, naive, marked data and independent output). The test is performed on a collection of marked sferics taken from a different set of data to that used for fitting the models. The procedure used to obtain each of the marked sferics is the same as that outlined in Sect. 5.1. The sferics are selected using a simple thresholding method (filtered sferics with a peak amplitude greater than a chosen threshold are selected).

Noise cancellation is performed by feeding marked sferics obtained at the reference antenna through the models to generate estimates of the marked sferics at the output antenna. The results are illustrated in Figs. 9 to 11. Fig. 9 shows the measured and estimated filtered outputs, and the residual errors for a single marked sferic. Fig. 10 shows the measured filtered output and residual errors

for the collection of marked sferics. The residual errors are offset from zero to separate the plots. The figures show that the residual errors for the non-stationary EIV, marked and independent output methods are similar in size, and are noticeably smaller than the residual error for the naive method. Fig. 11 shows the PSDs of the signals shown in Fig. 10, and confirms that the model found using the EIV method performs in a comparable fashion to the two validation models. All three of these models provide a significant reduction in the sferics noise mound.

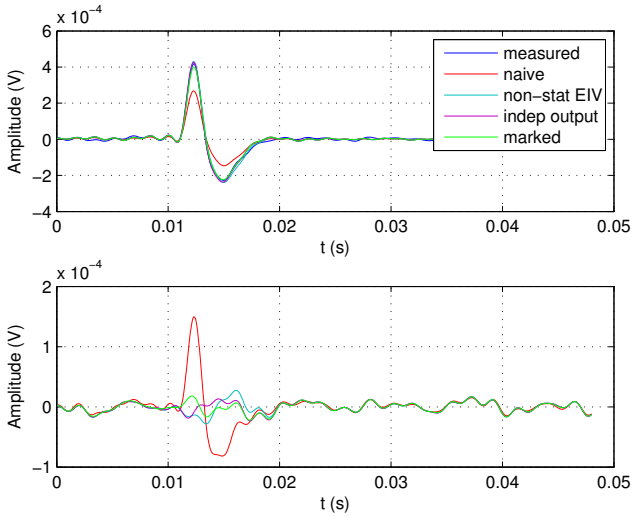


Fig. 9. Measured output, estimates of the output (top) and residual errors (bottom) for a single marked sferic.

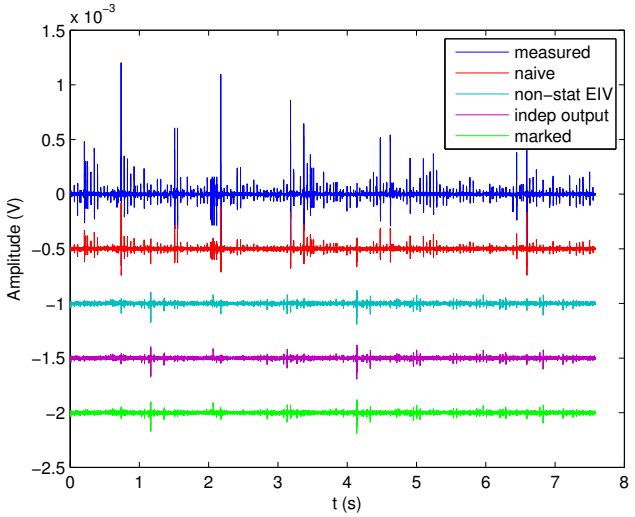


Fig. 10. Filtered sferics at the output (marked sferics) and residual errors when the fitted models are used for noise cancellation. The residuals are offset from zero to separate the plots.

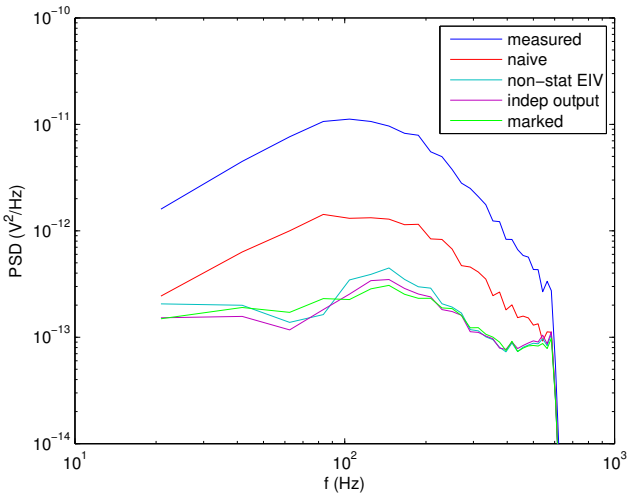


Fig. 11. PSDs of the signals shown in Fig. 10.

## 6 Conclusion

This paper has presented and applied a non-stationary errors-in-variables (EIV) model estimation method. The method has been validated by comparing its performance with two other methods (marked data, and independent output) which exploit specific features of the transient electromagnetic problem and are thus difficult to translate to other problems.

All three methods (i.e., non-stationary EIV, marked data and independent output) have been compared with a naive method which ignores the EIV issue and have been shown to yield superior performance for the intended noise cancellation problem.


## Acknowledgements

We would like to acknowledge J. Lee, M. Downey, R. Turner and A. Maddever, from BHP-Billiton for their contribution to this project. We especially thank J. Lee for proposing the problem and M. Downey for collecting the experimental data used in this paper.


## References


Agüero, J. C., Goodwin, G. C., 2008a. Identifiability of EIV dynamic systems with non-stationary data. In: Proceedings of the 17th IFAC World Congress. Seoul, Korea, pp. 444–449.

Agüero, J. C., Goodwin, G. C., 2008b. Identifiability of errors in variables dynamic systems. Automatica 44 (2), 371–382.

Anderson, B. D. O., 1985. Identification of scalar errors-in-variables models with dynamics. Automatica 21 (6), 709–716.

Anderson, B. D. O., Deistler, M., 1984. Identifiability in dynamic errors-in-variables model. Journal of Time Series Analysis 5 (1), 001–013.

Carter, R. A., 2005. Exploration by the numbers. Engineering and Mining Journal 206 (5), 34–38. URL www.scopus.com

Christian, H. J., Blakeslee, R. J., Boccippio, D. J., Boeck, W. L., Buechler, D. E., Driscoll, K., Goodman, S. J., Hall, J. M., Koshak, W. J., Mach, D. M., Stewart, M. F., Jan. 2003. Global frequency and distribution of lightning as observed from space by the optical transient detector. Journal of Geophysical Research 108, ACL4–1–15.

Deistler, M., 1986. Linear dynamic errors-in-variables models. Edited by J. Gani and M. B. Priestley. Journal of Applied Probability 23 (A), 23–39.

Kearney, P., Brooks, M., Hill, I., 2002. An introduction to geophysical exploration, 3rd Edition. Blackwell Science, Malden MA.

Lau, K., Braslavsky, J. H., Agüero, J. C., Goodwin, G. C., 2008. Application of non-stationary EIV methods to transient electromagnetic mineral exploration. In: Proceedings of the 17th IFAC World Congress. Seoul, Korea, pp. 438–443.

Lau, K., Braslavsky, J. H., Goodwin, G. C., 2007. Errors-in-variables problems in transient electromagnetic mineral exploration. In: Proceedings of the 46th IEEE Conference on Decision and Control. New Orleans, LA, USA.

Markovsky, I., Kukush, A., Van Huffel, S., 2006. On errors-in-variables estimation with unknown noise variance ratio. In: Preprints of the 14th IFAC Symposium in System Identification. Newcastle, Australia, pp. 172–177.

Nabighian, M. N., Macnae, J. C., 1991. Time domain electromagnetic prospecting methods. In: Nabighian, M. N. (Ed.), Electromagnetic Methods in Applied Geophysics Vol. 2, Application, Part A. Society of Exploration Geophysics, pp. 427–520.

Söderström, T., 2002. Discrete-Time Stochastic Systems: Estimation and Control, 2nd Edition. Springer-Verlag, London.

Söderström, T., 2007. Errors-in-variables methods in system identification. Automatica 43 (6), 939–958.

U.S. Army, 1998. Geophysical exploration for engineering and environmental investigations. Technical engineering and design guides as adapted from the U.S. Army Corps of Engineers No. 23. ASCE Press.

Wald, A., 1940. The fitting of straight lines if both variables are subject to error. Ann. Math. Stat. Series B. 11 (3), 284–300.